Supplemental Information

	Gene name	Allele name	Phenotype	Recessivity	Penetr-ance	Molecular Lesion	Reference
i	Mutations resulting in the absence of TRN maker						
	lin-32	*u909*	Lack of PLM, AVM, and PVM labeling	recessive	58%		Mitani et al., 1993
	cdk-4	*u948*	Lack of PLM, AVM, and PVM labeling	recessive	88%	Q18*	
	mec-4	*u947; u972*	Degeneration of TRNs	recessive	35% *(u947)*	A513T	
		u951	Degeneration of TRNs	dominant	65%	A713T	Driscoll and Chalfie, 1991
	mec-10	*u1025*	Degeneration of TRNs	recessive	10%	G312R	
ii	Mutations resulting in the expression of TRN markers in extra cells						
	egl-46	*u945*	Expression of TRN marker in FLPs	recessive	65%		Wu et al., 2001
	egl-44	*u965*	Expression of TRN marker in FLPs	recessive	79%		Wu et al., 2001
	pag-3	*u920; u949; u961*	Expression of TRN marker in BDUs	recessive	90% (*u920*)		Jia et al., 1996
	egl-13	*u964*	Expression of TRN marker in A/PQRs	recessive	68%	H389Y	Feng et al., 2013
iii	Mutations resulting in developmental defects in AVM/PVM						
	egl-20	*u999*	PVM is mispositioned anteriorly	recessive	82%	V92D	Harris et al., 1996
	unc-6	*u1018*	Ventral guidance defects for AVM neurites	recessive	61%	C346Y	Hedgecock et al., 1990

Table S1. Mutations that affect the expression pattern of TRN marker or the development of the postembryonic AVM and PVM cells. References indicate that similar mutant phenotypes for the gene were previously reported. *cdk-4* was not previously known to affect TRN development. Although they each have the same underlying defect, *u947* and *u972* were independently isolated. These two alleles and *mec-10(u1025)* identify novel changes that cause TRN degeneration.

	Gene name	Allele name	Recessivity	Penet-rance	Molecular Lesion	Reference
A	Mutations that shorten all TRN neurites					
	mec-7	*u910*	dominant	100%	P356L	
		u911	dominant		P171S	
		u955	dominant		A352T	
		u956	dominant		P358L	
		u957	dominant		P171L	
		u958	dominant		G244S	
	unc-51	*u1000*	recessive	80%	E188K	Du and Chalfie, 2001
B	Mutations that shorten the PLM-PN					
	mec-7	*u1020*	recessive		G34S	
	mec-12	*u1019*	dominant		G354E	
		u950	recessive		S140F	
		u1016	recessive		E97K	
		u1021	recessive		G144S	
	dsh-1	*u915*	recessive	95%	R165Stop	Zheng et al., 2015a
		u952	recessive		G512R	
		u953	recessive		R103Stop	
	tiam-1	*u914*	recessive	98%	R570Stop	Zheng et al., 2016
		u1003	recessive			
		u1004	recessive		R420Stop	
		u1005	recessive		Q846Stop	
		u1012	recessive		Q266Stop	
	egl-5	*u918; u966*	recessive	100%		Zheng et al., 2015b
	mua-3	*u973*	recessive	45%	C2191Y	
	sup-26	*u916*	recessive	81%	G95Stop	
C	Mutations that result in an ectopic ALM-PN					
	mec-12	*u917*	recessive	38%	V260I	
	mec-7	*u1017*	recessive	83%	L377F	
	tba-7	*u1015*	recessive	79%	G92D	
D	Mutations that shorten PLM-AN and elongate PLM-PN					
	lin-44	*u905; u906; u907; u959*	recessive	90% *(u905)*		Hilliard and Bargmann, 2006; Zheng et al., 2015a
	lin-17	*u919; u960; u962; u963*	recessive	75% *(u919)*		Hilliard and Bargmann, 2006; Zheng et al., 2015a
E	Mutations that shorten both PLM-AN and PLM-PN					
	mec-15	*u1008*	recessive	83%	Q194Stop	
F	Mutations that shorten ALM-AN and PLM-AN					
	unc-73	*u908*	recessive	85%	E1212K	Du and Chalfie, 2001; Zheng et al., 2016
	unc-53	*u913*	recessive	90%	Q261Stop	Hekimi and Kershaw, 1993
		u912; u946; u967; u968; u969; u970; u971; u974	recessive			
	klp-11	*u1024*	recessive	79%	Q53Stop	
G	Mutations that shorten ALM-AN but not PLM-AN					
	unc-23	*u1022*	recessive	82%	Q132Stop	

Table S2 Mutations that cause neurite outgrowth or guidance defects in TRNs. References indicate that the similar mutant phenotypes for the gene were either previously reported or we extensively characterized the mutants elsewhere.

Gene	Allele	TRN morphology
tba-1	*ok1123*	Normal
tba-1	*ok1135*	Normal
tba-1	*or346*	Normal
tba-1	*or594*	Normal
tba-2	*sb51*	Normal
tba-2	*sb25*	Normal
tba-5	*tm4200*	Normal
tba-7	*gk787939*	Ectopic ALM-PN
tba-7	*u1015*	Ectopic ALM-PN
tba-8	*tm4359*	Normal
tba-9	*ok1858*	Normal
ben-1	*e1880*	Normal
tbb-1	*gk207*	Normal
tbb-2	*t1623*	Normal
tbb-2	*gk130*	Normal
tbb-4	*sa127*	Normal
tbb-4	*ok1461*	Normal
tbb-6	*tm2004*	Normal

Table S3. Loss-of-function alleles of α and β tubulin genes (other than *mec-12* and *mec-7*) and their effects on TRN morphology.

Gene name	Mutation	Structural function	Corpus Callosum	Reference
TUBA1A	I5L	Tubulin folding	hypoplastic CC	Jansen et al., 2011
	E55K	Lumen-facing loop	partial ACC	Morris-Rosendahl et al., 2008
	T56M	Lumen-facing loop	complete ACC	Bahi-Buisson et al., 2014
	L70S	GTP binding	complete ACC	Cushion et al., 2013
	P72S	Intradimer interaction	hypoplastic CC	Bahi-Buisson et al., 2014
	L92V	Lumen-facing loop	complete ACC	Kumar et al., 2010
	N101S	GTP binding	complete ACC	Bahi-Buisson et al., 2014
	E113K	Lateral interaction	Normal	Bahi-Buisson et al., 2014
	R123C	Lateral interaction	Normal	Bahi-Buisson et al., 2014
	V137D	Tubulin folding	partial ACC	Kumar et al., 2010
	S158L	Tubulin folding	complete ACC	Bahi-Buisson et al., 2014
	Y161H	Lateral interaction	hypoplastic CC	Poirier et al., 2013
	I188L	Tubulin folding	partial ACC	Poirier et al., 2007
	Y210C	Intradimer interaction	hypoplastic CC	Jansen et al., 2011
	R214H	Intradimer interaction	complete ACC	Bahi-Buisson et al., 2014
	D218Y	Intradimer interaction	complete ACC	Kumar et al., 2010
	I219V	Intradimer interaction	partial ACC	Oegema et al., 2015
	V235L	Tubulin folding	hypoplastic CC	Poirier et al., 2013
	I238V	Tubulin folding	complete ACC	Fallet-Bianco et al., 2008
	D249H	Longitudinal interaction	complete ACC	Poirier et al., 2007
	P263T	MAP binding	complete ACC	Fallet-Bianco et al., 2008
	R264H	MAP binding	complete ACC	Bahi-Buisson et al., 2014
	R264C	MAP binding	Normal	Poirier et al., 2007
	A270T	Tubulin folding	complete ACC	Kumar et al., 2010
	L286F	Lateral interaction	complete ACC	Fallet-Bianco et al., 2008
	V303G	Tubulin folding	partial ACC	Lecourtois et al. 2010
	R320H	Tubulin folding	partial ACC	Bahi-Buisson et al., 2014
	K326N	Longitudinal interaction	complete ACC	Bahi-Buisson et al., 2014
	N329S	Longitudinal interaction	complete ACC	Kumar et al., 2010
	A333V	Longitudinal interaction	hypoplastic CC	Cushion et al., 2013
	V353I	Longitudinal interaction	partial ACC	Bahi-Buisson et al., 2014
	G366R	Lumen-facing loop	partial ACC	Okumura et al. 2013
	A369T	Lumen-facing loop	hypoplastic CC	Bahi-Buisson et al., 2014
	V371E	Lumen-facing loop	complete ACC	Bahi-Buisson et al., 2014
	M377V	Tubulin folding	partial ACC	Kumar et al., 2010
	A387V	MAP binding	hypoplastic CC	Romaniello et al., 2012
	R390C	MAP binding	complete ACC	Kumar et al., 2010
	R390H	MAP binding	partial ACC	Zanni et al. 2013
	D396Y	MAP binding	partial ACC	Bahi-Buisson et al., 2014
	L397P	MAP binding	partial ACC	Bahi-Buisson et al., 2008
	R402L	MAP binding	mild hypoplastic CC	Sohal et al., 2012
	R402C	MAP binding	normal	Kumar et al., 2010
	R402H	MAP binding	normal	Kumar et al., 2010
	V409A	MAP binding	complete ACC	Bahi-Buisson et al., 2014
	V409I	MAP binding	hypoplastic CC	Bahi-Buisson et al., 2014
	S419L	MAP binding	partial ACC	Poirier et al., 2007
	R422H	MAP binding	partial ACC	Kumar et al., 2010

	R422C	MAP binding	hypoplastic CC	Bahi-Buisson et al., 2008
	M425K	MAP binding	complete ACC	Kumar et al., 2010
	E429Q	MAP binding	complete ACC	Bahi-Buisson et al., 2014
	G436R	MAP binding	hypoplastic CC	Bahi-Buisson et al., 2008
TUBB2B	G13A	Tubulin folding	normal	Oegema et al., 2015
	G98R	GTP binding	complete ACC	Cushion et al., 2013
	L117P	Tubulin folding	normal	Guerrini et al., 2012
	G140A	GTP binding	complete ACC	Romaniello et al., 2012
	P171T	GTP binding	partial ACC	Bahi-Buisson et al., 2014
	S172P	GTP binding	complete ACC	Jaglin et al., 2009
	P173L	GTP binding	complete ACC	Bahi-Buisson et al., 2014
	I202T	Tubulin folding	partial ACC	Bahi-Buisson et al., 2014
	L207P	Tubulin folding	complete ACC	Cushion et al., 2013
	I210T	Tubulin folding	partial ACC	Jaglin et al., 2009
	L228P	Tubulin folding	complete ACC	Jaglin et al., 2009
	C239F	Intradimer interaction	complete ACC	Bahi-Buisson et al., 2014
	R241H	Intradimer interaction	normal	Bahi-Buisson et al., 2014
	A248T	Intradimer interaction	normal	Bahi-Buisson et al., 2014
	D249H	Intradimer interaction	complete ACC	Bahi-Buisson et al., 2014
	N256S	Intradimer interaction	hypoplastic CC	Guerrini et al., 2012
	F265L	Tubulin folding	partial ACC	Jaglin et al., 2009
	S278G	Lateral interaction	partial ACC	Bahi-Buisson et al., 2014
	T312M	Tubulin folding	hypoplastic CC	Jaglin et al., 2009
	G369V	Lumen-facing loop	partial ACC	Bahi-Buisson et al., 2014
	R380S	MAP binding	complete ACC	Cushion et al., 2013
	R380C	MAP binding	complete ACC	Cushion et al., 2013
	R380L	MAP binding	complete ACC	Amrom et al., 2014
	D417N	MAP binding	normal	Guerrini et al., 2012
TUBB3	R46G	Intradimer interaction	hypoplastic CC	Bahi-Buisson et al., 2014
	R62Q	Tubulin folding	normal	Tischfield et al., 2010
	G71R	Tubulin folding	partial ACC	Whitman et al., 2016
	G82R	Tubulin folding	partial ACC	Poirier et al., 2010
	G98S	Longitudinal interaction	hypoplastic CC	Whitman et al., 2016
	T178M	GTP binding	complete ACC	Poirier et al., 2010
	E205K	Tubulin folding	hypoplastic CC	Poirier et al., 2010
	R262C	MAP binding	partial ACC	Tischfield et al., 2010
	R262H	MAP binding	partial ACC	Tischfield et al., 2010
	E288K	Lateral interaction	hypoplastic CC	Oegema et al., 2015
	A302T	MAP binding	partial ACC	Tischfield et al., 2010
	A302V	MAP binding	hypoplastic CC	Poirier et al., 2010
	M323V	Intradimer interaction	partial ACC	Poirier et al., 2010
	P357L	Tubulin folding	normal	Oegema et al., 2015
	R380C	MAP binding	partial ACC	Tischfield et al., 2010
	M388V	MAP binding	complete ACC	Poirier et al., 2010
	E410K	MAP binding	partial ACC	Tischfield et al., 2010
	D417N	MAP binding	partial ACC	Tischfield et al., 2010
	D417H	MAP binding	N/A	Tischfield et al., 2010

Table S4. Missense mutations in human α and β tubulins that caused neurological disorders in heterozygous patients. 51 TUBA1A, 24 TUBB2B, and 19 TUBB3B mutations are listed. The mutated amino acids were mapped to the structural domains of α/β heterodimer and their potential structural functions were assigned according to Tischfield *et al.* (2011). Residues located in the interior of the structure were generally assigned to the category of "tubulin folding." Effects on the corpus callosum (CC) were used as an indicator of defects in axon growth and guidance. These phenotypes were extracted from the cited literature. ACC stands for agenesis of the corpus callosum.

Supplemental Figures

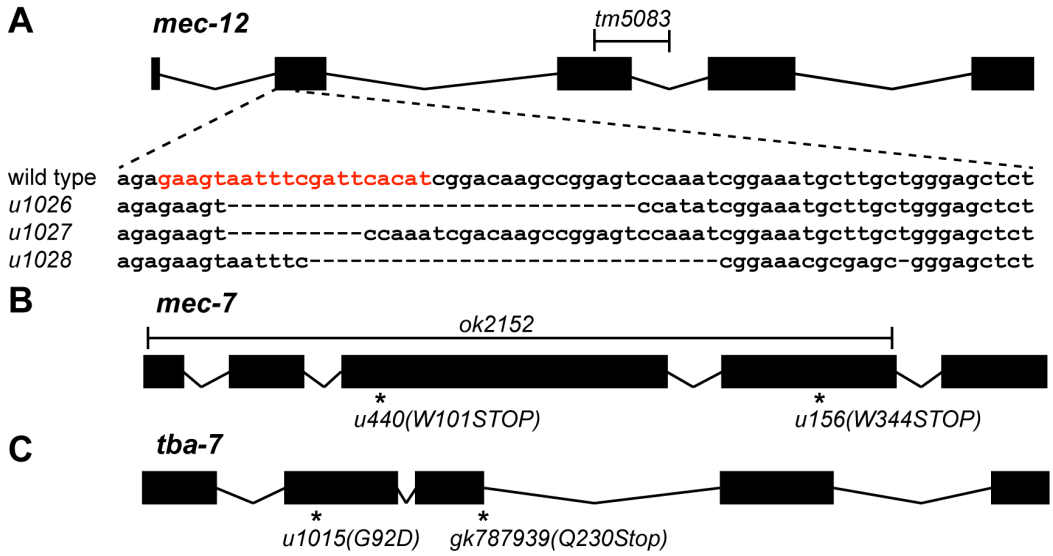

Figure S1. Gene structures for *mec-12*, *mec-7*, and *tba-7* and the molecular lesions in various putative null alleles. *u1026*, *u1027*, and *u1028* were created using CRISPR/Cas9-mediated genome editing and guide RNAs designed to target exon 2 of *mec-12*. Frameshift-causing deletions were identified by genotyping. The *tm5083* mutation deletes part of exon 3 and intron 3 of *mec-12* and also causes a frameshift.

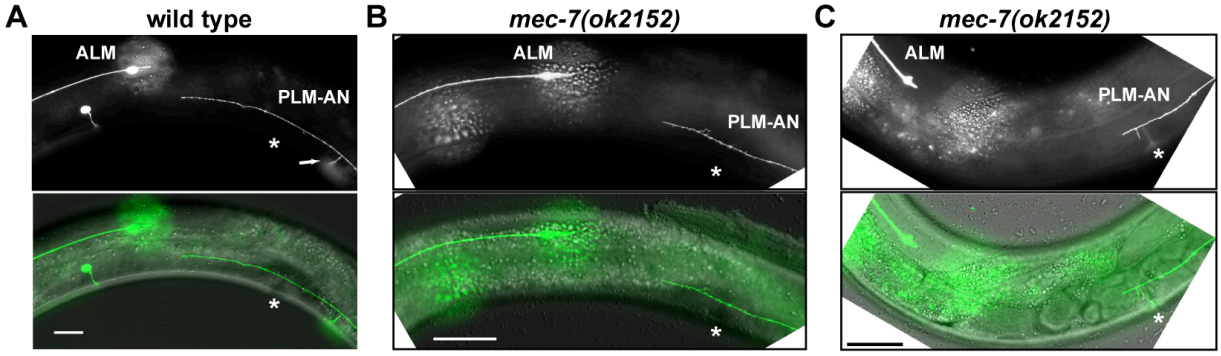

Figure S2. The loss of MEC-7 causes PLM-AN branching defects. (A) In the wild-type animals, PLM-AN extends beyond the vulva (asterisk) and sends out a synaptic branch at a position posterior to the vulva; the branch extends to reach the ventral nerve cord. (B-C) PLM-AN is slightly shorter in *mec-7 (ok2152lf)* animals, although it still extends beyond the vulva (triangle). However, PLM-AN fails to form a synaptic branch (B) or could not fully extend the branch at the correct position (C).

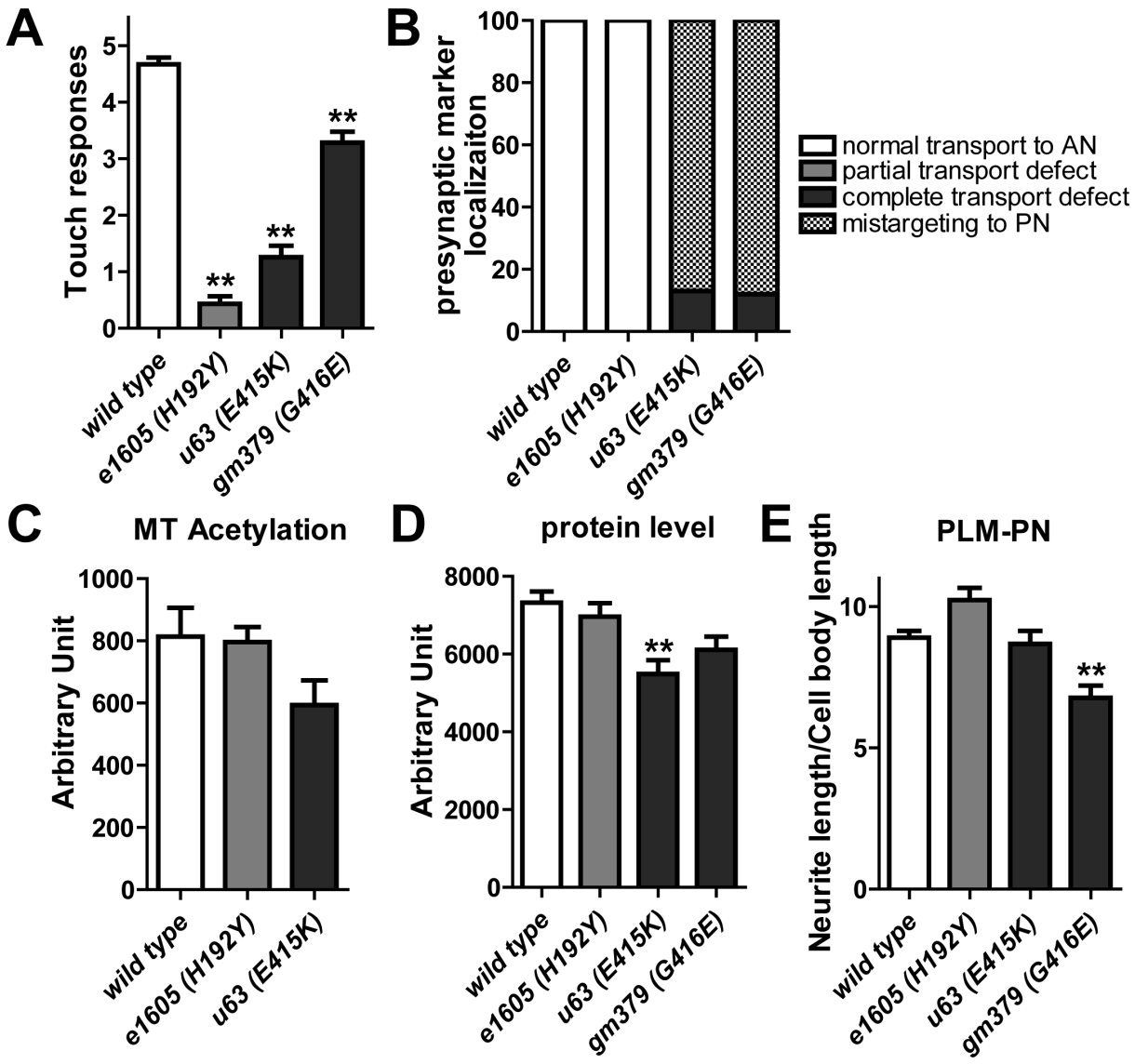

Figure S3. *mec-12* alleles that specifically affect touch sensitivity or synaptic vesicle transport. (A) Anterior touch response (out of five stimuli) of the *mec-12* alleles. (B) Percentage of PLM cells showing transport defects or mistargeting of the presynaptic marker RAB-3::GFP. (C) Immunofluorescent intensity of staining using anti-acetylated α-tubulin antibodies. (D) Fluorescent intensity of RFP expressed from the transgene *uIs134[mec-17p::RFP]* crossed into the *mec-12* mutants. Arbitrary units were used in C and D. (E) The length of the PLM-PN in some *mec-12* mutants. Asterisks indicate significant differences ($p < 0.01$) from the wild type animals.

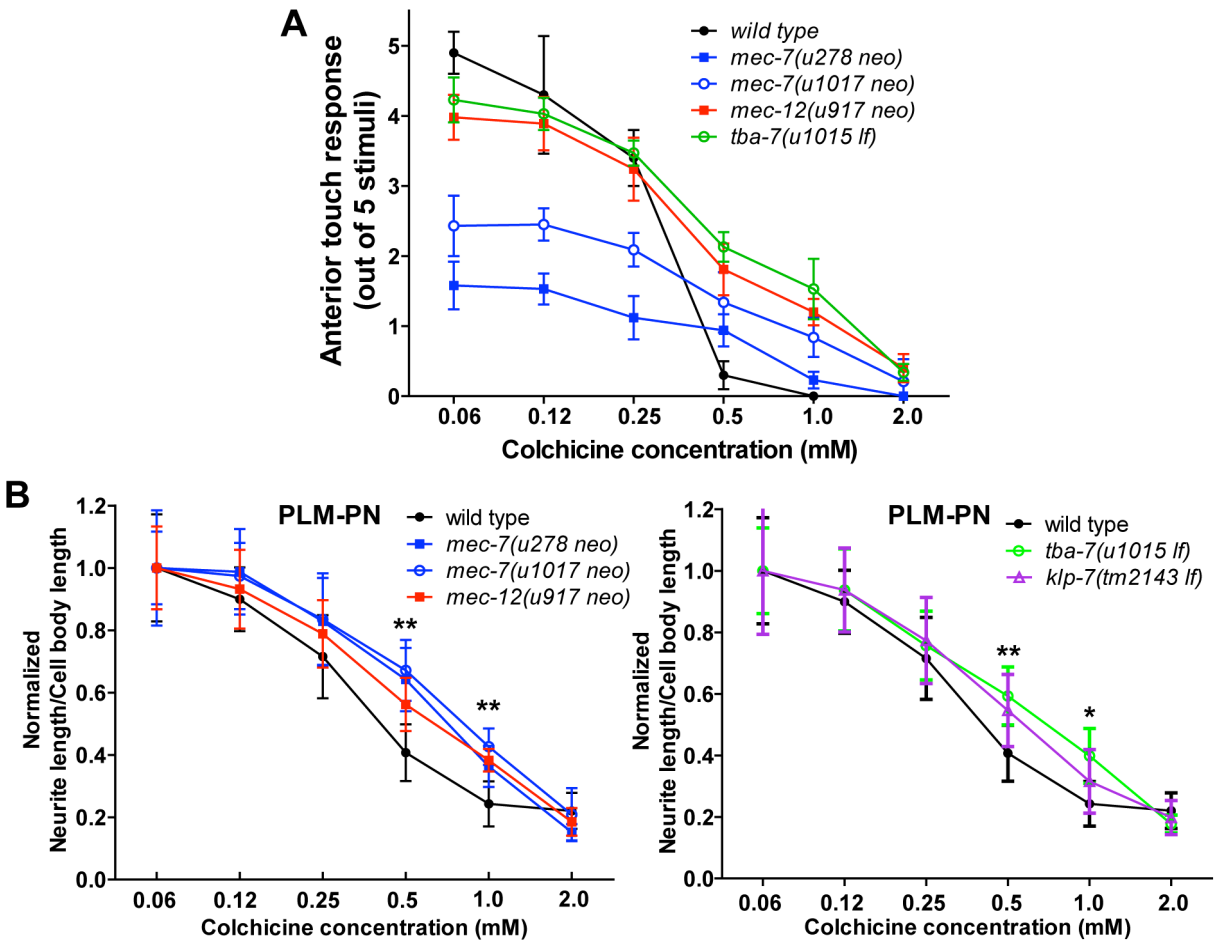

Figure S4. *mec-7(neo)* and *mec-12(neo)*, *tba-7(lf)*, and *klp-7(lf)* mutants have increased resistance to colchicine. (A) Anterior touch response of adult animals grown on plate containing different concentrations of colchicine from the first larval (L1) stage. (B) The normalized length of PLM-PN of adults grown on plates with colchicine from the L1 stage. PLM-PN lengths of animals treated with 0.06 mM colchicine (9.0 for wild type, 13.3 for *u278*, 10.0 for *u1017*, 10.1 for *u917*, 11.0 for *u1015*, and 10.5 for *tm2143*) were used to set as the reference for the normalization. Asterisks indicate the differences among the means were statistically significant in ANOVA tests (one asterisk indicates $p < 0.05$ and two for $p < 0.01$).

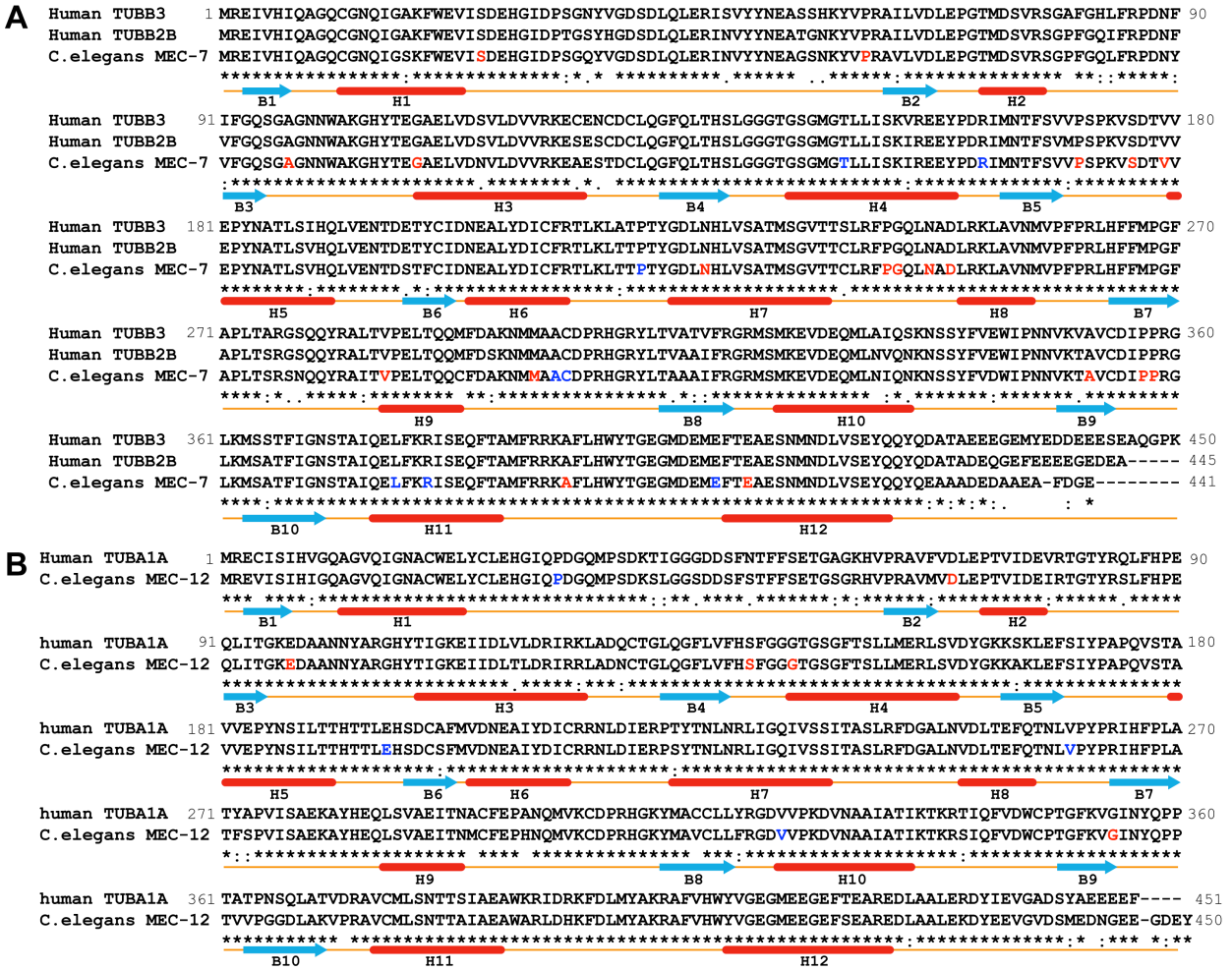

Figure S5. Sequence alignment of MEC-7 with human TUBB3 and TUBB2B (A) and alignment between MEC-12 and TUBA1A (B). Regions predicted to be α-helices (H1 to H12) or β-strands (B1 to B10) by the α/β tubulin dimer structure (1jff.pdb; Nogales et al. 1998) were labeled. Amino acids that were changed in *mec-7* or *mec-12* antimorphs and neomorphs were labeled in red and blue, respectively.

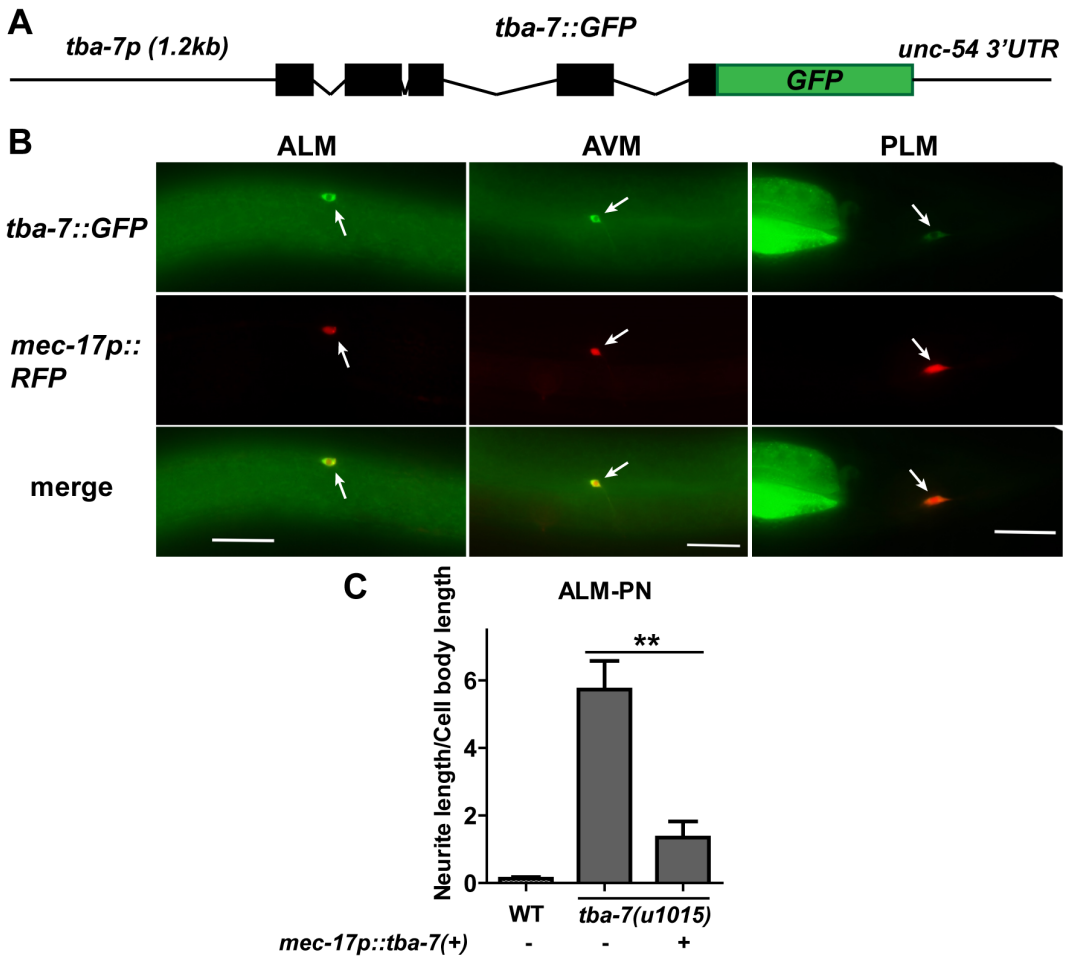

Figure S6. TBA-7 is expressed and acts cell-autonomously in the TRNs. (A) A schematic representation of the *tba-7::GFP* reporter, containing a 1.2 kb promoter and the entire coding region. (B) The expression of *tba-7::GFP* in the TRNs, which are also labeled by *mec-17p::RFP*. Arrows point to the cell bodies of TRNs. The posterior intestine also showed strong GFP signal (the rightmost panel). (C) The length of ALM-PN in *tba-7(u1015 lf)* mutants that carried a rescuing array that expressed wild-type *tba-7* in the TRNs specifically.

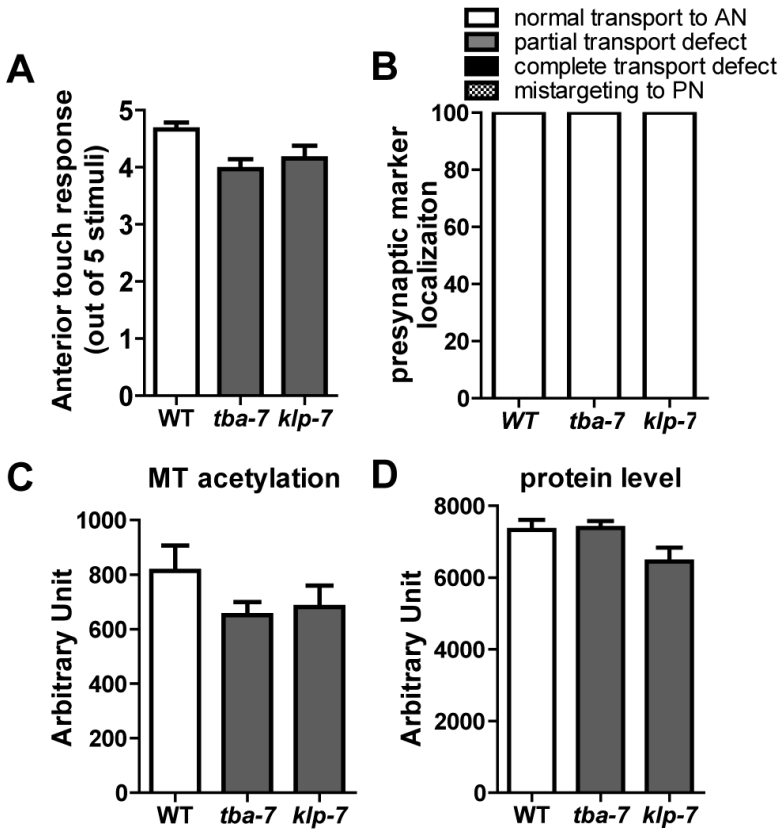

Figure S7. Touch sensitivity, presynaptic vesicle localization, tubulin acetylation level, and protein expression level of *tba-7(u1015 lf)* and *klp-7(tm2143 lf)* mutants. No significant differences between these mutants and wild type were found.

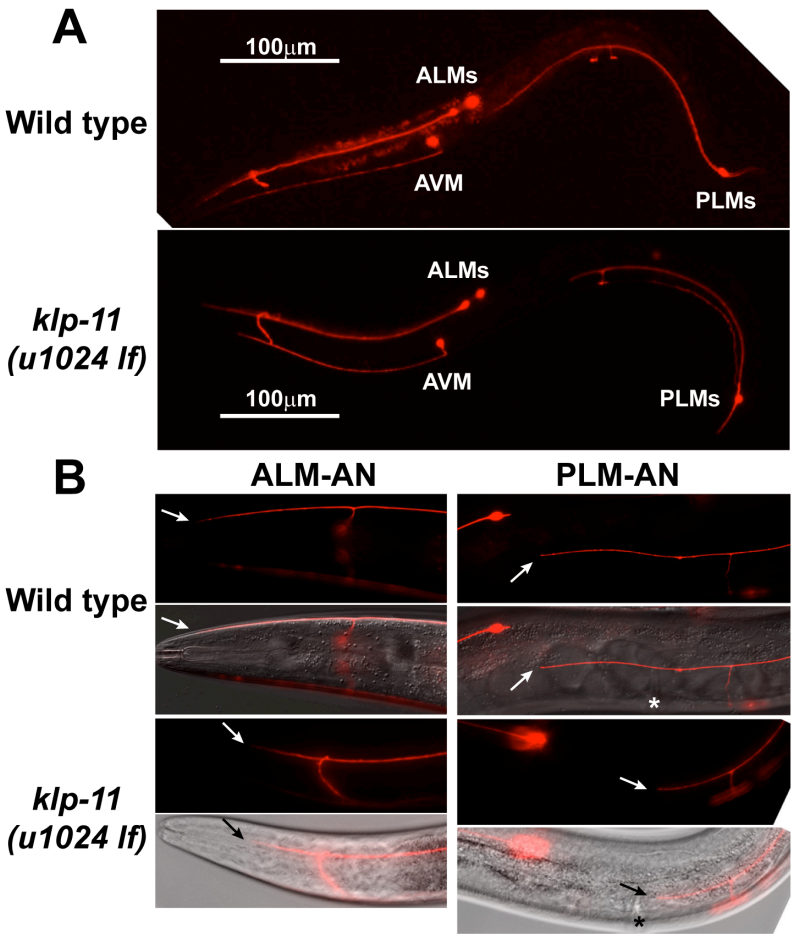

Figure S8. Moderate shortening of ALM-AN and PLM-AN in *klp-11[u1024* (Q53*) *lf]* mutants. In (B), arrows point to the ends of the anterior neurites, and triangles indicate the position of the vulva. ALM-AN did not extend as far as the procorpus of the pharynx and PLM-AN failed to reach the vulva in *klp-11* mutants.

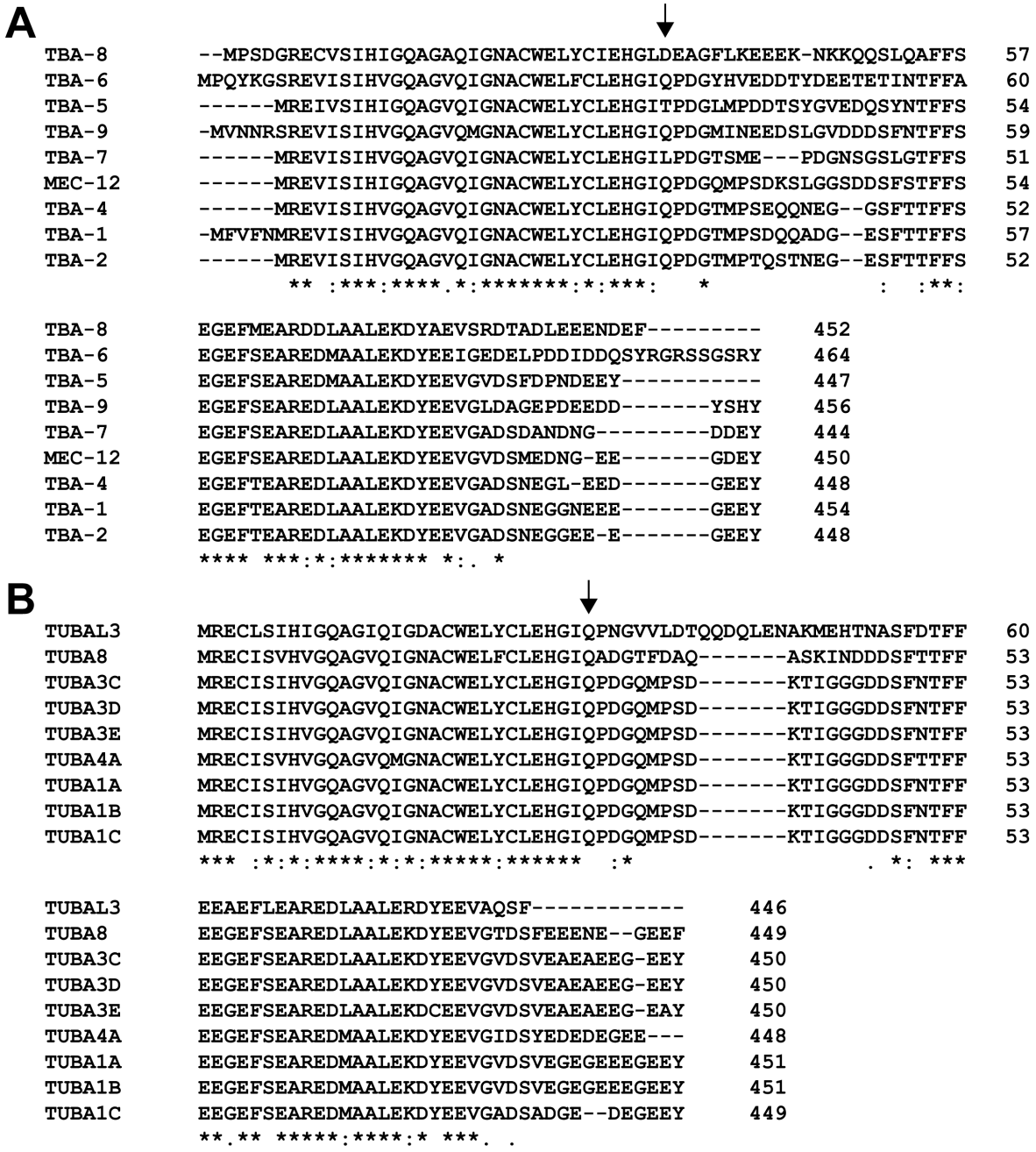

Figure S9. Sequence alignment of all *C. elegans* α-tubulin proteins (A) and all human α-tubulin proteins (B). Only the N-terminal and C-terminal sequences were shown. The arrow points to Q31 residue.

References

Amrom D, Tanyalcin I, Verhelst H, Deconinck N, Brouhard GJ, Decarie JC, Vanderhasselt T, Das S, Hamdan FF, Lissens W et al. 2014. Polymicrogyria with dysmorphic basal ganglia? Think tubulin! *Clin Genet* **85**: 178-183.

Bahi-Buisson N, Poirier K, Boddaert N, Saillour Y, Castelnau L, Philip N, Buyse G, Villard L, Joriot S, Marret S et al. 2008. Refinement of cortical dysgeneses spectrum associated with TUBA1A mutations. *J Med Genet* **45**: 647-653.

Bahi-Buisson N, Poirier K, Fourniol F, Saillour Y, Valence S, Lebrun N, Hully M, Bianco CF, Boddaert N, Elie C et al. 2014. The wide spectrum of tubulinopathies: what are the key features for the diagnosis? *Brain* **137**: 1676-1700.

Cushion TD, Dobyns WB, Mullins JG, Stoodley N, Chung SK, Fry AE, Hehr U, Gunny R, Aylsworth AS, Prabhakar P et al. 2013. Overlapping cortical malformations and mutations in TUBB2B and TUBA1A. *Brain* **136**: 536-548.

Driscoll M, Chalfie M. 1991. The mec-4 gene is a member of a family of Caenorhabditis elegans genes that can mutate to induce neuronal degeneration. *Nature* **349**: 588-593.

Du H, Chalfie M. 2001. Genes regulating touch cell development in Caenorhabditis elegans. *Genetics* **158**: 197-207.

Fallet-Bianco C, Loeuillet L, Poirier K, Loget P, Chapon F, Pasquier L, Saillour Y, Beldjord C, Chelly J, Francis F. 2008. Neuropathological phenotype of a distinct form of lissencephaly associated with mutations in TUBA1A. *Brain* **131**: 2304-2320.

Feng G, Yi P, Yang Y, Chai Y, Tian D, Zhu Z, Liu J, Zhou F, Cheng Z, Wang X et al. 2013. Developmental stage-dependent transcriptional regulatory pathways control neuroblast lineage progression. *Development* **140**: 3838-3847.

Guerrini R, Mei D, Cordelli DM, Pucatti D, Franzoni E, Parrini E. 2012. Symmetric polymicrogyria and pachygyria associated with TUBB2B gene mutations. *Eur J Hum Genet* **20**: 995-998.

Harris J, Honigberg L, Robinson N, Kenyon C. 1996. Neuronal cell migration in C. elegans: regulation of Hox gene expression and cell position. *Development* **122**: 3117-3131.

Hedgecock EM, Culotti JG, Hall DH. 1990. The unc-5, unc-6, and unc-40 genes guide circumferential migrations of pioneer axons and mesodermal cells on the epidermis in C. elegans. *Neuron* **4**: 61-85.

Hekimi S, Kershaw D. 1993. Axonal guidance defects in a Caenorhabditis elegans mutant reveal cell-extrinsic determinants of neuronal morphology. *The Journal of neuroscience : the official journal of the Society for Neuroscience* **13**: 4254-4271.

Hilliard MA, Bargmann CI. 2006. Wnt signals and frizzled activity orient anterior-posterior axon outgrowth in C. elegans. *Developmental cell* **10**: 379-390.

Jaglin XH, Poirier K, Saillour Y, Buhler E, Tian G, Bahi-Buisson N, Fallet-Bianco C, Phan-Dinh-Tuy F, Kong XP, Bomont P et al. 2009. Mutations in the beta-tubulin gene TUBB2B result in asymmetrical polymicrogyria. *Nat Genet* **41**: 746-752.

Jansen AC, Oostra A, Desprechins B, De Vlaeminck Y, Verhelst H, Regal L, Verloo P, Bockaert N, Keymolen K, Seneca S et al. 2011. TUBA1A mutations: from isolated lissencephaly to familial polymicrogyria. *Neurology* **76**: 988-992.

Jia Y, Xie G, Aamodt E. 1996. pag-3, a Caenorhabditis elegans gene involved in touch neuron gene expression and coordinated movement. *Genetics* **142**: 141-147.

Kumar RA, Pilz DT, Babatz TD, Cushion TD, Harvey K, Topf M, Yates L, Robb S, Uyanik G, Mancini GM et al. 2010. TUBA1A mutations cause wide spectrum lissencephaly (smooth brain) and suggest that multiple neuronal migration pathways converge on alpha tubulins. *Hum Mol Genet* **19**: 2817-2827.

Lecourtois M, Poirier K, Friocourt G, Jaglin X, Goldenberg A, Saugier-Veber P, Chelly J, Laquerriere A. 2010. Human lissencephaly with cerebellar hypoplasia due to mutations in TUBA1A: expansion of the foetal neuropathological phenotype. *Acta Neuropathol* **119**: 779-789.

Mitani S, Du H, Hall DH, Driscoll M, Chalfie M. 1993. Combinatorial control of touch receptor neuron expression in Caenorhabditis elegans. *Development* **119**: 773-783.

Morris-Rosendahl DJ, Najm J, Lachmeijer AM, Sztriha L, Martins M, Kuechler A, Haug V, Zeschnigk C, Martin P, Santos M et al. 2008. Refining the phenotype of alpha-1a Tubulin (TUBA1A) mutation in patients with classical lissencephaly. *Clin Genet* **74**: 425-433.

Nogales E, Wolf SG, Downing KH. 1998. Structure of the alpha beta tubulin dimer by electron crystallography. *Nature* **391**: 199-203.

Oegema R, Cushion TD, Phelps IG, Chung SK, Dempsey JC, Collins S, Mullins JG, Dudding T, Gill H, Green AJ et al. 2015. Recognizable cerebellar dysplasia associated with mutations in multiple tubulin genes. *Hum Mol Genet* **24**: 5313-5325.

Okumura A, Hayashi M, Tsurui H, Yamakawa Y, Abe S, Kudo T, Suzuki R, Shimizu T, Shimojima K, Yamamoto T. 2013. Lissencephaly with marked ventricular dilation, agenesis of corpus callosum, and cerebellar hypoplasia caused by TUBA1A mutation. *Brain Dev* **35**: 274-279.

Poirier K, Keays DA, Francis F, Saillour Y, Bahi N, Manouvrier S, Fallet-Bianco C, Pasquier L, Toutain A, Tuy FP et al. 2007. Large spectrum of lissencephaly and pachygyria phenotypes resulting from de novo missense mutations in tubulin alpha 1A (TUBA1A). *Hum Mutat* **28**: 1055-1064.

Poirier K, Saillour Y, Bahi-Buisson N, Jaglin XH, Fallet-Bianco C, Nabbout R, Castelnau-Ptakhine L, Roubertie A, Attie-Bitach T, Desguerre I et al. 2010. Mutations in the neuronal ss-tubulin subunit TUBB3 result in malformation of cortical development and neuronal migration defects. *Hum Mol Genet* **19**: 4462-4473.

Poirier K, Saillour Y, Fourniol F, Francis F, Souville I, Valence S, Desguerre I, Marie Lepage J, Boddaert N, Line Jacquemont M et al. 2013. Expanding the spectrum of TUBA1A-related cortical dysgenesis to Polymicrogyria. *Eur J Hum Genet* **21**: 381-385.

Romaniello R, Tonelli A, Arrigoni F, Baschirotto C, Triulzi F, Bresolin N, Bassi MT, Borgatti R. 2012. A novel mutation in the beta-tubulin gene TUBB2B associated with complex malformation of cortical development and deficits in axonal guidance. *Dev Med Child Neurol* **54**: 765-769.

Sohal AP, Montgomery T, Mitra D, Ramesh V. 2012. TUBA1A mutation-associated lissencephaly: case report and review of the literature. *Pediatr Neurol* **46**: 127-131.

Tischfield MA, Baris HN, Wu C, Rudolph G, Van Maldergem L, He W, Chan WM, Andrews C, Demer JL, Robertson RL et al. 2010. Human TUBB3 mutations perturb microtubule dynamics, kinesin interactions, and axon guidance. *Cell* **140**: 74-87.

Tischfield MA, Cederquist GY, Gupta ML, Jr., Engle EC. 2011. Phenotypic spectrum of the tubulin-related disorders and functional implications of disease-causing mutations. *Curr Opin Genet Dev* **21**: 286-294.

Whitman MC, Andrews C, Chan WM, Tischfield MA, Stasheff SF, Brancati F, Ortiz-Gonzalez X, Nuovo S, Garaci F, MacKinnon SE et al. 2016. Two unique TUBB3 mutations cause both CFEOM3 and malformations of cortical development. *Am J Med Genet A* **170A**: 297-305.

Wu J, Duggan A, Chalfie M. 2001. Inhibition of touch cell fate by egl-44 and egl-46 in C. elegans. *Genes & development* **15**: 789-802.

Zanni G, Colafati GS, Barresi S, Randisi F, Talamanca LF, Genovese E, Bellacchio E, Bartuli A, Bernardi B, Bertini E. 2013. Description of a novel TUBA1A mutation in Arg-390 associated with asymmetrical polymicrogyria and mid-hindbrain dysgenesis. *Eur J Paediatr Neurol* **17**: 361-365.

Zheng C, Diaz-Cuadros M, Chalfie M. 2015a. Dishevelled attenuates the repelling activity of Wnt signaling during neurite outgrowth in Caenorhabditis elegans. *Proceedings of the National Academy of Sciences of the United States of America* **112**: 13243-13248.

-. 2015b. Hox Genes Promote Neuronal Subtype Diversification through Posterior Induction in Caenorhabditis elegans. *Neuron* **88**: 514-527.
-. 2016. GEFs and Rac GTPases control directional specificity of neurite extension along the anterior-posterior axis. *Proceedings of the National Academy of Sciences of the United States of America* **113**: 6973-6978.